The International Journal of Advanced Manufacturing Technology (2019) 102:507–518
https://doi.org/10.1007/s00170-018-03210-y

ORIGINAL ARTICLE

Fiber orientations effect on process performance for wire cut electrical discharge machining (WEDM) of 2D C/SiC composite

Wenbin He[1] · Shaotai He[1] · Jinguang Du[1] · Wuyi Ming[1] · Jun Ma[1] · Yang Cao[1] · Xiaoke Li[1]

Received: 22 July 2018 / Accepted: 13 December 2018 / Published online: 4 January 2019

Abstract

Adopting orthogonal experiments, relevant machinability in wire cut electrical discharge machining (WEDM) of 2D C/SiC composite was studied. The effects of electrical machining parameters (namely pulse width, pulse interval, and the number of tubes) on machining speed and surface roughness were analyzed. In addition, the effect of fiber orientations on the machinability was also studied. The main effect and interaction of the selected electrical machining parameters were also discussed. The key results show that the fiber orientation effect on machining speed plays a weaker role in WEDM of this composite. For machining speed, the number of tubes and the pulse interval have no interaction in both of machining directions A and B. For surface roughness, the number of tubes and the pulse interval have obvious interaction in both of machining directions A and B. The fiber orientation has a larger effect on the surface roughness than that on machining speed in WEDM of this composite. After analyzing the material removal mechanism, some new significant results show that the carbon fibers are removed in the form of transverse and longitudinal fracture. Interfacial debonding between fiber carbon and SiC matrix, pit, and recast layer form on the machined surface. Micro cracks are observed in the carbon fiber, and a part of the micro cracks are cross.

Keywords C/SiC composite · Fiber orientation · Wire cut electrical discharge machining · Machining speed · Surface roughness

1 Introduction

C/SiC composites are a kind of high-performance composite materials that are manufactured by SiC ceramic as a matrix with carbon fiber as reinforcement. [1]. In view of its excellent properties, for instance, low specific gravity, high hardness, small thermal expansion coefficient, etc., has a wide application prospect in the aerospace field [2].

As a kind of difficult-to-machine material, C/SiC composites easily produce machining deficiency, such as layered failure, edge breakage, delamination, and machined surface damage. For the past few years, there are some studies on the conventional machining methods of C/SiC composite such as grinding [3], milling [4, 5], and drilling [6, 7]. However, due to the brittleness and hardness of the composites, the aforementioned traditional machining has serious tool wear and poor processing quality. There is no better solution for machining small-diameter deep holes for grinding and/or drilling this composites.

The non-traditional machining methods, such as electric spark machining, laser machining, and rotational ultrasonic machining, have been adopted to machine C/SiC composites, which can avoid the disadvantages of some

✉ Jinguang Du
dujinguangzzuli@163.com

Wenbin He
hwbzzuli@163.com

Shaotai He
m15639782009@163.com

Wuyi Ming
mwyzzuli@163.com

Jun Ma
majun@zzuli.edu.cn

Yang Cao
caoy@163.com

Xiaoke Li
lxkzzuli@163.com

[1] Henan Provincial Key Laboratory of Intelligent Manufacturing of Mechanical Equipment, Zhengzhou University of Light Industry, Zhengzhou 450002, China

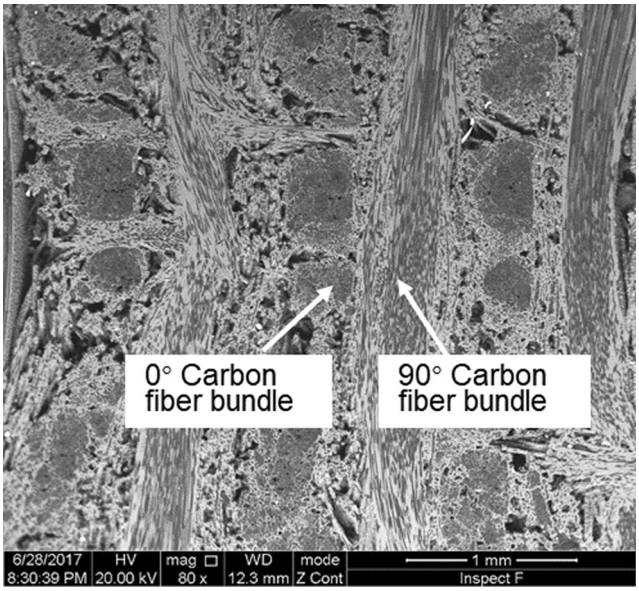

Fig. 1 SEM image of composite used [22]

Table 1 Main property of C/SiC composite [22]

Properties (at room temperature)	Parameters
Density (g/cm^3)	1.7
Flexural strength (MPa)	181
Compressive strength ∥ (MPa)	210
Compressive strength ⊥ (MPa)	245
Interlaminar shear strength (MPa)	19–21
Tensile strength at room temperature (MPa)	100
Thermal conductivity (W/m K)	5–6.3
Coefficient of thermal expansion ($\times 10^{-6}$ K)	1.1–2.5

traditional machining methods and has unique advantages in machining of feature structures. Some scholars have studied the non-traditional methods and their performance in the machining of C/SiC composites. Ha et al. studied the energy-controlled micro-discharge machining of Al_2O_3-carbon nanotube composites and analyzed the relationship between hardness and electrical conductivity [8]. Ninz et al. analyzed the correlation between the metallic nanoscale inclusions and mechanical properties of ED-machinability and zirconia-TiC-based ceramics by means of EDM of nanocomposites [9]. Kumar et al. compared the results of processing Al-SiC_p MMC with conventional electrical discharge machining (CEDM) and cryogenic cooling EDM (CCEDM) and found that CCEDM is superior to CEDM [10]. Saxena et al. studied the material removal process, surface quality, and SiC migration by studying the micro-EDM process [11]. Using rotary ultrasonic machining, Wang et al. analyzed the change of fiber breakage with tool vibration for machining of C/SiC composites [12]. Saxena et al. studied different machining parameters on the processability of micro-EDM SiC and found that capacitance, voltage, and threshold all had a significant influence on the experiment objective, namely MRR, TWR, surface roughness, and ROC [13]. Wu et al. performed a comparative analysis of the micro surface morphology using laser-ablated unidirectional fiber end orientation of C/SiCs [14]. Ding et al. adopted a rotary ultrasonic and conventional drilling of C/SiC composites to study the cutting force and machined surface quality [15]. Ji et al. had done electric discharge milling experiments of SiC ceramic with a tool electrode made by steel-toothed wheel [16]. Liu et al. applied single line and spiral scanning methods to analyze the changes in the processing characteristics with laser energy density in picosecond laser C/SiC composites [17]. Zhang et al. probed that fiber orientations have influence when surface grinding 2D C/SiC composites [18]. A novel monitoring method was found by Diaz et al., which is helpful in analyzing the type of crack formation appearing during machining of CMCs [19]. Wang et al. investigated a new ultrasonic vibration filing (UVF) for inner surface machining of C/SiC composites. The cutting force and surface quality are analyzed and compared with common grinding (CG) and common filing (CF) [20]. Liao et al. studied the effect of anisotropy of bone on the chip formation in orthogonal cutting and explained

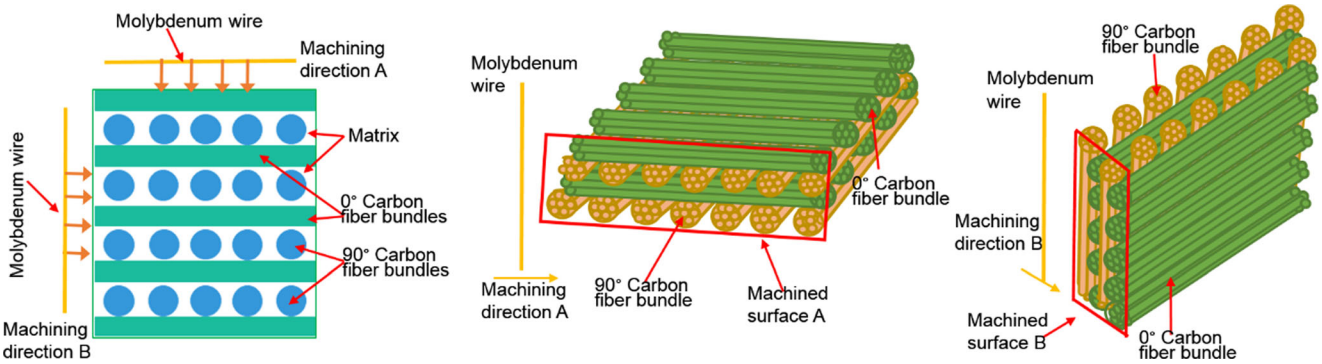

Fig. 2 Sketch map of carbon fiber orientation relative to machining directions

Table 2 Main parameters of wire electrical discharge machine

Parameters	Range/values
Table travel	320 mm × 400 mm
Working fluid	Mixed saponified liquid
Pulse width	10–300 us
Pulse interval	2–16 ns
Number of tubes	2–15
Pulse power supply	GD-8
Maximum cutting thickness	300 mm

Table 3 Orthogonal factor level for WEDM

Factors	Pulse width A/(us)	Pulse interval B/(ns)	Number of tubes C
1	20	4	4
2	40	6	6
3	60	8	8
4	80	10	10

the chip morphologies in different bone fibers considered in the model. This study can provide a reference for machining C/SiC composite [21].

At present, traditional machining methods have been adopted to machining the 2D-C/SiC composite with woven structure. At each the same layer, the carbon fiber (0° and 90°) are simultaneously orthogonally weaved. Although ceramic and ceramic matrix composites have been studied through non-traditional machining methods, a few interesting conclusions are drawn out. However, very little study has been made in the respect of the fiber orientation's effect on the machinability in wire cut electrical discharge machining (WEDM) of 2D C/SiC composites. It includes 0° and 90° carbon fiber that are weaved at two different structure sheaf, respectively. Based on related experiments in WEDM of 2D C/SiC composite, this study focuses the fiber orientation and electrical parameters' effects on the machinability, namely, machining speed and surface roughness. The influence of machining direction relative to fiber orientations is considered. Besides, the material removal mechanism in WEDM, this C/SiC composite was also explained. This study also attempts to obtain some novel and valuable conclusions to promote the processing efficiency in WEDM of this composite.

2 Experimental procedure

2.1 Experimental material

The adopted material fabricated by chemical vapor infiltration in this study contains 65% carbon reinforcement of fiber and 30% silicon carbide matrix). Figure 1 shows the microstructure SEM image of the composite used that shows each layer with a thickness of about 350 μm weaved with one direction carbon fiber bundles. Around the carbon fibers is the matrix material. The weaved 0° or 90° carbon fiber is spread over in two different layers, respectively. Table 1 shows the main property of C/SiC composite.

Table 4 Orthogonal experimental arrangement

Serial number	A Pulse width (μs)	B Pulse interval (ns)	C Number of tubes	Peak current (A)
1	20	4	4	2.3
2	20	6	6	2.5
3	20	8	8	2.6
4	20	10	10	2.7
5	40	4	6	3.5
6	40	6	4	1.7
7	40	8	10	3.3
8	40	10	8	2.1
9	60	4	8	4.7
10	60	6	10	4.2
11	60	8	4	1.3
12	60	10	6	1.6
13	80	4	10	6.0
14	80	6	8	3.4
15	80	8	6	2.0
16	80	10	4	1.0

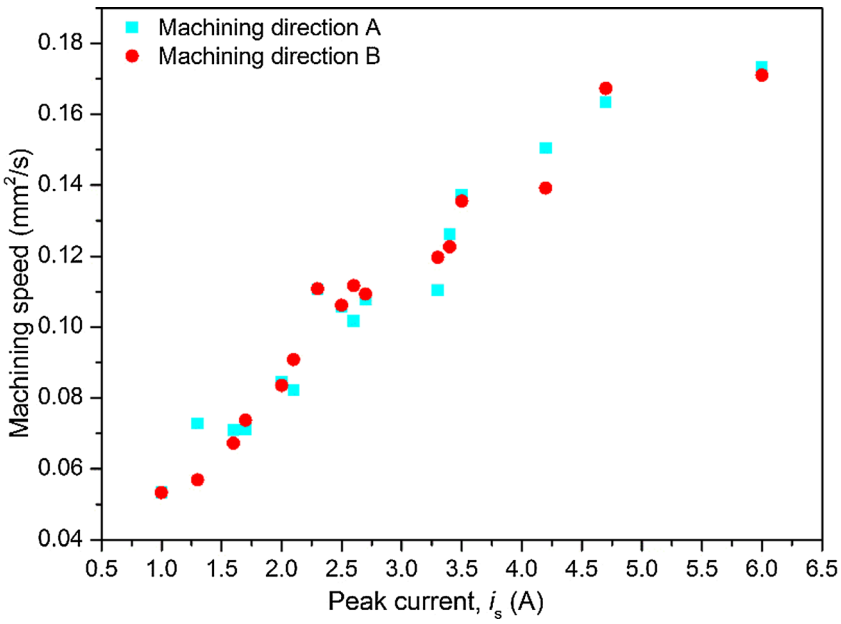

Fig. 3 Effect of peak current on machining speed (M.S.)

2.2 WEDM process

Given the woven structure of this material, the orientation of carbon fiber in the two layers is orthogonal. Figure 2 shows the sketch map of carbon fiber orientation relative to machining directions. Due to adjacent two different layers of composites exiting different orientation of the carbon fibers, machining directions A and B as shown in Fig. 2 have different effects on the machinability of WEDM in this material.

The machining direction A (in machined surface A) represents that the feed direction of molybdenum wire is consistent with the 0° carbon fiber orientation, and simultaneously perpendicular to the 90° carbon fiber orientation. The machining direction B (in machined surface B) represents that the feed of molybdenum wire was perpendicular to both 0°and 90° carbon fiber orientations. The effects of the electrical parameters (pulse width, pulse interval, and a number of tubes) on the machining speed (M.S.) and 3D surface roughness (Sa) were explained, and the removal process of carbon fiber was also studied in conclusion.

2.3 Experiment design

A WEDM machine (DK7732E) was used to carry out experimental tests. The main wire electrical discharge machine parameters are given in Table 2. The used molybdenum wire is with a diameter of about 0.18 mm.

The orthogonal design is adopted in this study because it is an effective method that is used in the experimental study of various factors and various levels. In this design, some representative points that are evenly distributed are selected from the comprehensive test for the experiment according to its orthogonality. According to the machine tool used in these experiments, the pulse width, pulse interval, and the number of tubes were chosen as electrical machining parameters and factors based on an extensive literature survey. The number of tubes is one of the controlled input variables of the WEDM machine tool used in this study. It represents the discharge current as one of the common parameters. For this WEDM machine tool, one number of tubes denote discharged current of 1 A. The peak current is mainly decided by the pulse width, pulse interval, and the number of tubes. Four levels of each of the parameter were selected. The orthogonal experiment L_9 (3^4) was arranged to carry out the experiments to study their effects on machining speed and surface roughness. Table 3 gives the orthogonal factor level and Table 4 is the orthogonal experimental arrangement for WEDM.

The machining speed is the area of the workpiece cutoff in the unit time. The area of the workpiece is the same in all of

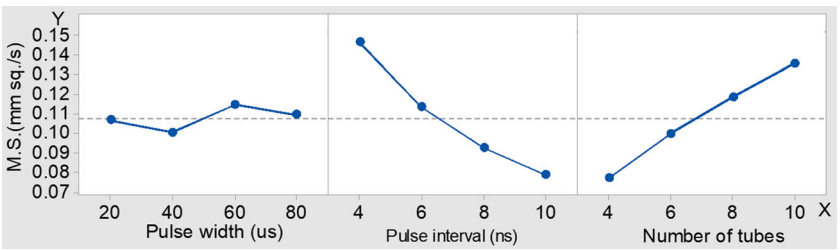

Fig. 4 Main effect plot for machining speed at machining direction A

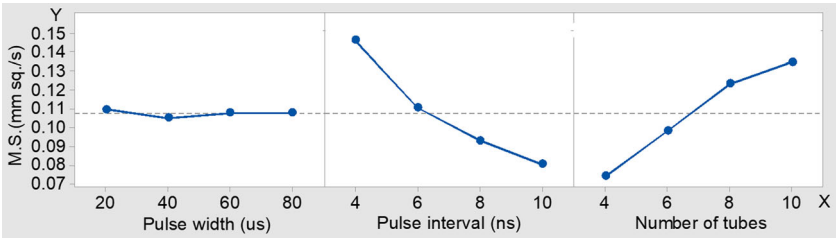

Fig. 5 Main effect plot for machining speed at machining direction B

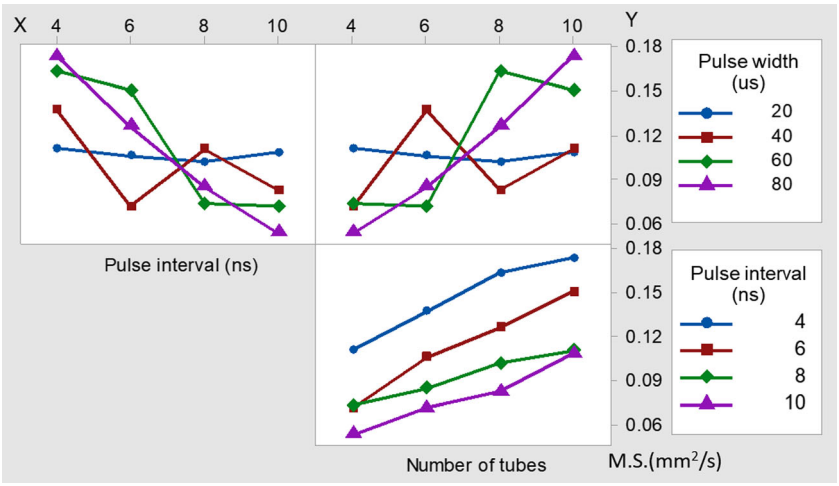

Fig. 6 The interaction plot of machining speed at machining direction A

the experiments. The machining time can be read out by the electric spark control system. Because of the anisotropy of the material, it is not accurate in characterizing a machined surface feature of C/SiC composite with the two-dimensional surface profile parameters (Ra). In contrast, the three-dimensional surface roughness parameter (Sa) contains more outline information, so the three-dimensional surface roughness (Sa) was used to evaluate the surface profile. The white light interferometer named Talysurf CCI 6000 from Taylor Hobson Company is applied to collect contour data. The WED machined surface morphology can be obtained from a scanning electron microscope (Quanta 250FEG from FEI Company).

3 Results and discussions

3.1 Cutting speed

The peak current is one of the major factors that determine the single pulse energy. Figure 3 gives the influence of peak current on machining speed (M.S.). It is observed that when the

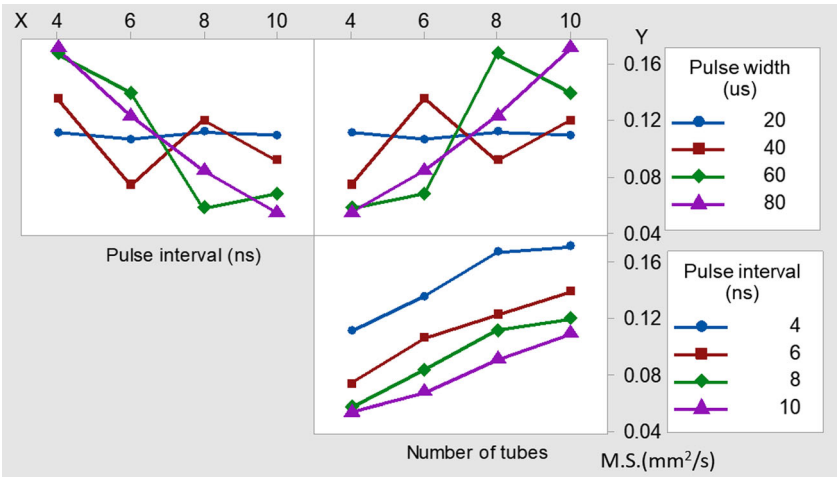

Fig. 7 The interaction plot of machining speed at machining direction B

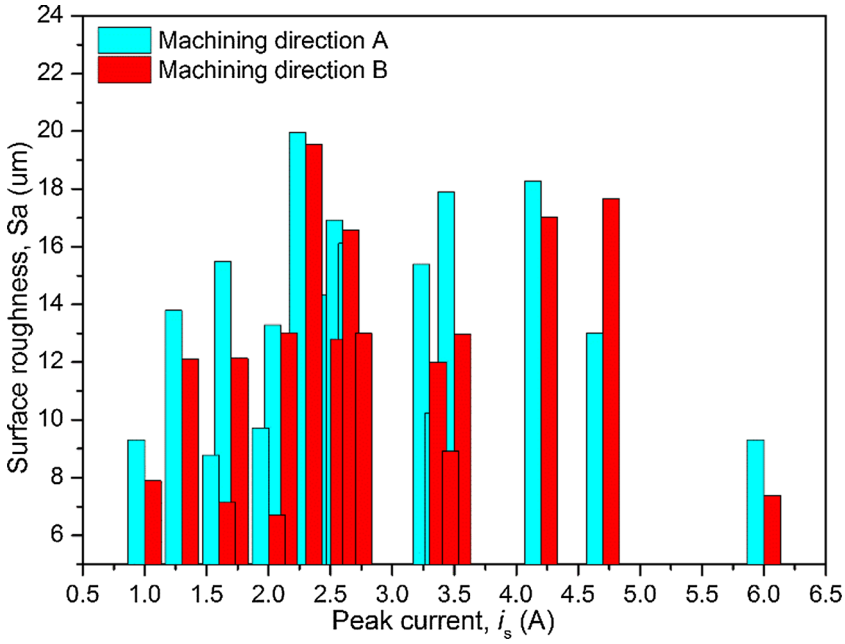

Fig. 8 Change of surface roughness (Sa) with peak current

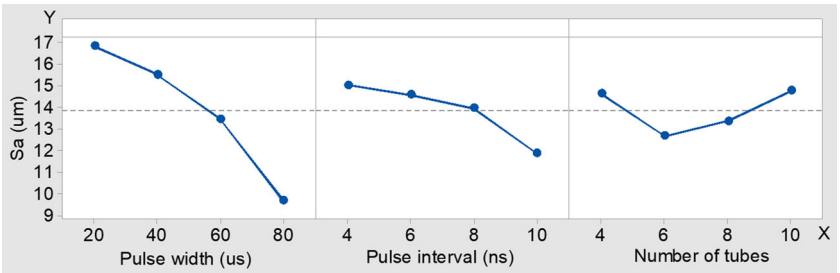

Fig. 9 Main effect plot of surface roughness at machining direction A

peak current is increasing, the machining speeds increase for two machining directions A and B. This is because increasing the peak current can enlarge the single pulse energy. The discharge mark increases and the machining speeds increase. From Fig. 3, it is also observed that the slope of the machining speed is faster at small peak current than that at large peak current for both two machining directions A and B. The main reasons can be attributed to the increase of the weeny debris produced in electric spark discharge at large peak current. The superabundant weeny debris is not removed in time. The machining speed is a little higher at large peak current at machining direction A than that at machining direction B. At small peak current, the fiber orientation effect on the machining speed plays a weaker role in WEDM of 2D C/SiC composite. It is also observed that owning to the shielding effect of SiC matrix, the machining speed is slower in WEDM of C/SiC composite than that of the traditional metal material.

The main effect plot for machining speed is given in Figs. 4 and 5 at machining directions A and B, respectively. With that plot, it can be drawn on how one or more categorical factors influence the continuous response. If the curve is not parallel to the x axial, there are main effects in the parameter variables.

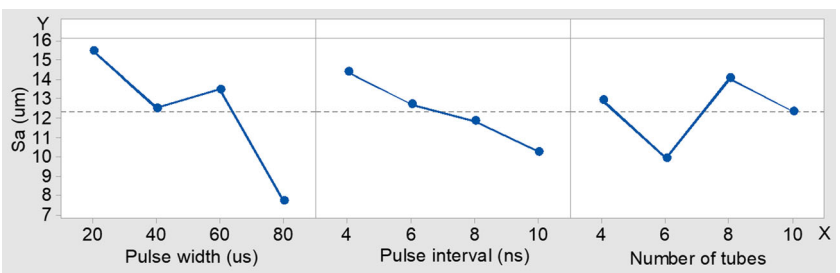

Fig. 10 Main effect plot of surface roughness at machining direction B

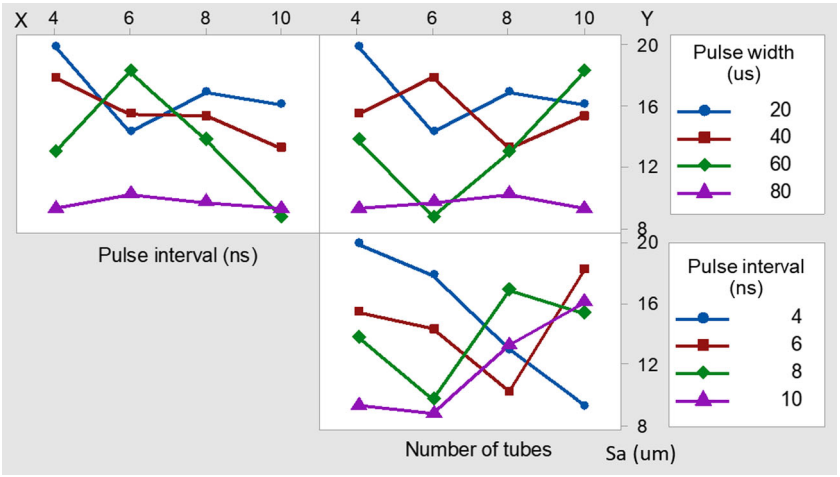

Fig. 11 The interaction plot of machining speed at machining direction A

The main effect degree increases with the increase of steepness of the curve.

From Figs. 4 and 5 in WEDM of this composite, it is here seen that the pulse interval and the number of tubes are significant for machining speed at machining directions A and B. With regard to the pulse power supply used in this study, when pulse interval decreases or the number of tubes increases, the peak current directly rises. And then the machining speed increases. The smaller the pulse interval, the more the number of discharge machining in unit time is. As the number of the tubes increases, the current and voltage also increase. For all the above reasons, the machining speed also increases. At the machining direction of A, at the pulse width of 60 us, the pulse interval of 4 ns, and the number of tubes of 10, the machining speed can get a larger value. At the machining direction B, the electrical parameters are the pulse width of 20 us, pulse interval of 4 ns, and number of tubes of 10.

Figures 6 and 7 give the interaction plot in WEDM of 2D C/SiC composite, respectively. The interaction plots are used to describe the dynamic cooperative relationships between one factor and another actor. The parallel line in the interaction plot indicates that there does is no exit interaction. If the difference slope between lines is greater, the interaction degree is also higher. From Figs. 6 and 7, it can be seen that the relationship between the pulse interval and machining speed relies on the pulse width. The relationship between the number of tubes and machining speed relies on the pulse width for both of the machining directions A and B. That is to say, using pulse interval of 4 ns, pulse width of 80 us can obtain the highest value of the machining speed. However, using the pulse interval of 10 ns, the pulse width of 20 us is also associated with the highest mean machining speed. The significant interaction occurs between the number of tubes and the pulse width. However, the number of tubes and the pulse interval have no obvious interaction for both of the machining directions A and B.

3.2 Surface roughness

Figure 8 gives the change of surface roughness (Sa) with peak current on at machining directions A and B, which revealed that as a whole, the surface roughness firstly increases at a

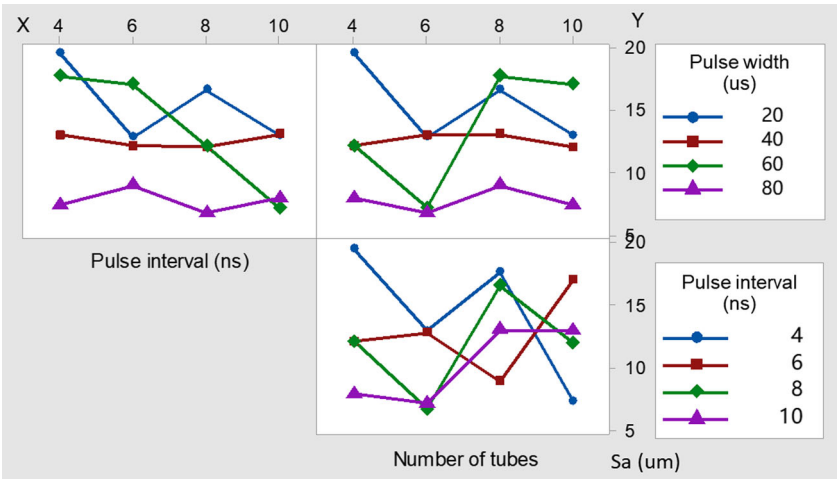

Fig. 12 The interaction plot of machining speed at machining direction B

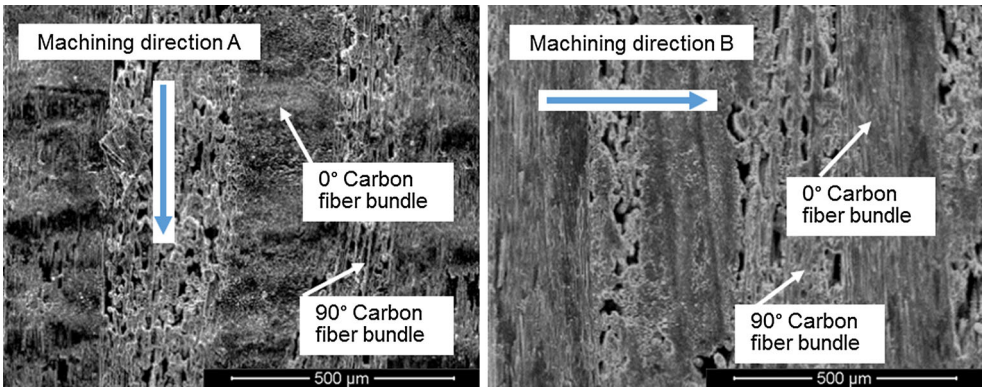

Fig. 13 Surface topography in WEDM of 2D C/SiC composite at the pulse width of 20 us, the pulse interval of 4 ns, and the number of tubes of 4

small peak current and then decreases as the peak current increases for both machining directions A and B. When the peak current increases, the single pulse energy enlarges, leading to a larger discharge mark and recast layer forming in the machined surface, so the surface roughness increases. When the peak current exceeds 4.0 A, the surface roughness begins to decline. As the peak current increases, the part of the formed recast layer would be gasified. The majority of Sa gained at machining direction A is higher than that gained at direction B. It is also observed from Fig. 13 of the surface topography in WEDM of 2D C/SiC composite at machining directions A and B, and also it can be seen that there exits obvious discharge trench in the 0° carbon fiber bundle of the machined surface.

Figures 9 and 10 represent the main effects plot of surface roughness at machining directions A and B, respectively. Unlike the main effect of the machining speed, pulse width has the most significant influence on surface roughness. With

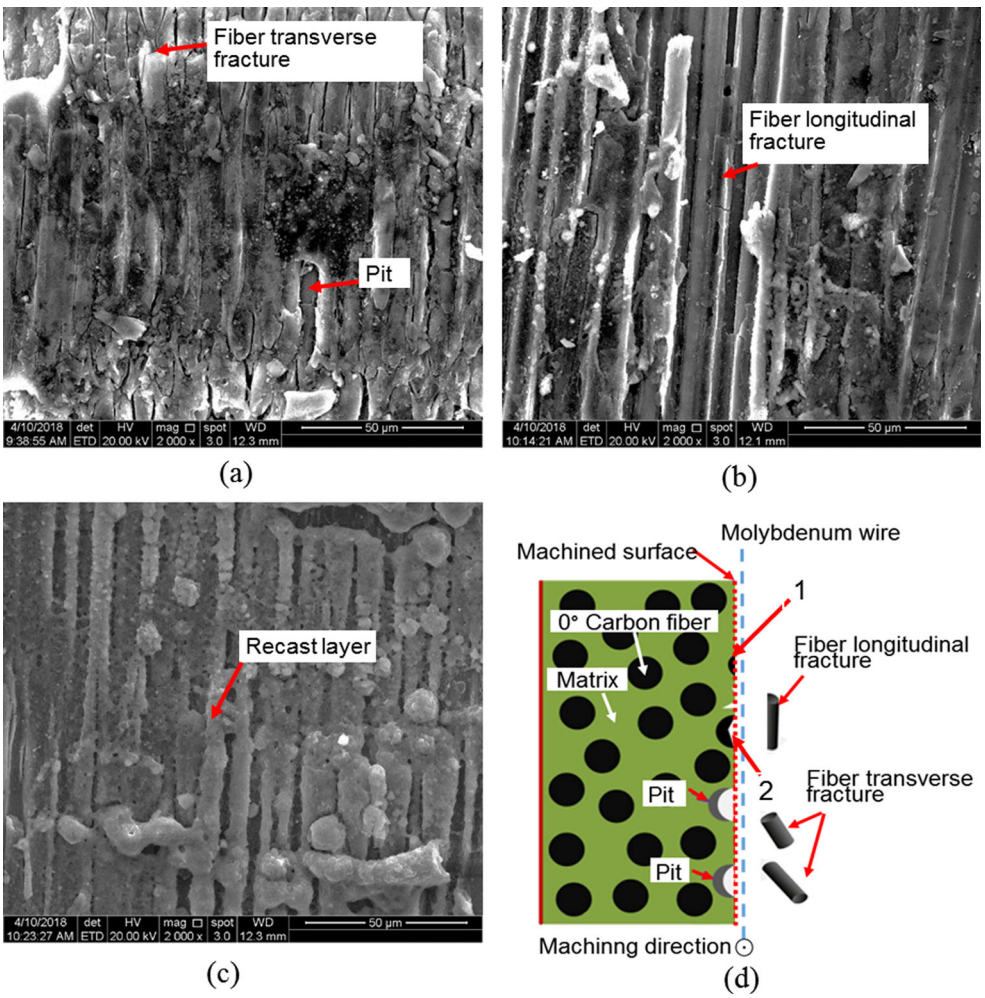

Fig. 14 Surface morphology and material removal progress using machining direction A

the increases of pulse width, the surface roughness shows a decreasing trend. The increase of the pulse width can make the discharge time of the single pulse becomes longer, which results in the local temperature rising. The amount of the machining for side edge increases and the produced heat emanates fast. With the pulse interval increasing, the surface roughness also decreases. This can be attributed to the reduction of pulse frequency and the decrease of discharge machining number per unit time. For both of directions A and B, the effect of the number of tubes on smaller roughness has a lot of volatility, which also indicates that the orientation of carbon fiber has an important influence on the material removal in WEDM of this composites. It can be also figured out that smaller roughness values can be gained under the pulse width of 80 us, the pulse interval of 10 ns, and the number of tubes of six. Figures 11 and 12 show the interaction plot of different electrical parameters at the directions A and B in the machining of this composite, respectively. Unlike the interaction plot of the machining speed, the data lines are all nonparallel lines, which means interaction is occurring. The number of tubes and pulse interval has an obvious interaction for both of the machining directions. The fiber orientation has a larger influence degree on the surface roughness than that on the machining speed in machining this composite.

3.3 Material removal mechanism

The anisotropy of this 2D composite results in different material removal mechanism from ordinary metal materials. Some special machining features will appear on the machined surface. Figure 13 shows the surface topography in WEDM of these composites at machining directions A and B using the pulse width of 20 us, pulse interval of 4 ns, and the number of tubes of four. It can be observed that there are many discharge traces in the machined surface at machining direction A. This is because WEDM composite at direction A can lead to the discharge traces left along the fiber direction. It also further explains that the majority of Sa gained at machining direction A is higher than that gained at the machining direction B in Fig. 8.

According to Fig. 2 and Zhang's study [18], there are three relative position relationships between machining direction and 0°/90° carbon fiber given in Figs. 14d, 15d, and 16d. Figure 14 gives surface morphology and material removal

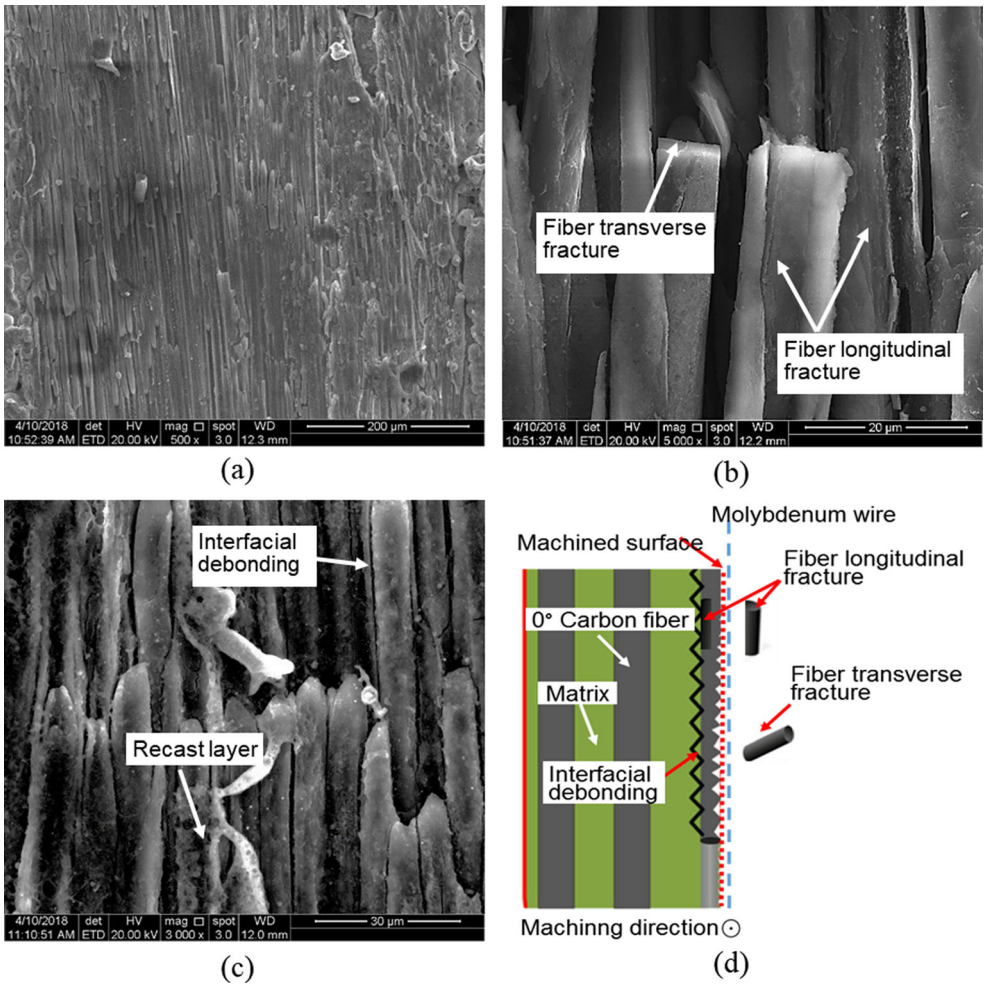

Fig. 15 Surface morphology and material removal progress using machining direction A

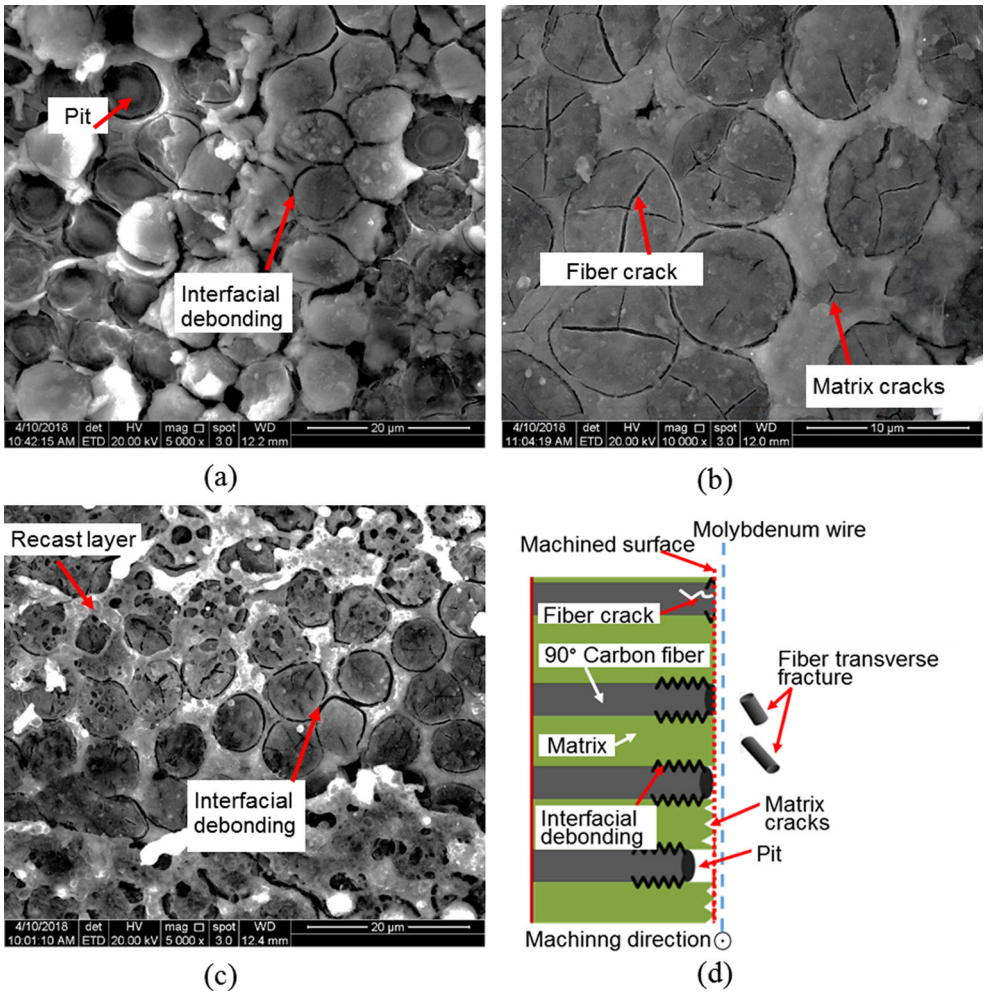

Fig. 16 Surface morphology and material removal progress using machining direction B

progress using machining direction A. It can be seen that the cut direction of the wire electrode is parallel to the 0° fiber bundle. As shown in Fig. 14a, during the spark discharge process, the carbon fiber produces the transverse fracture and then breaks off from a whole carbon fiber due to the action of pulse interval. And this also implies that the relative positional relation between the wire electrode and fiber has an important effect on the material removal mechanism. When the wire electrode cuts off a large proportion of the carbon fiber along its radial direction such as carbon fiber 1 in Fig. 14d, the action of the impact force and gasification produces by the microburst in the process of discharge. So, at the moment, the carbon fiber easily occurs transverse fracture, and the carbon fiber/SiC interface is damaged simultaneously. When the fractured carbon fiber falls off from a whole one then the pit forms, as shown in Fig. 14a. Figure 14b illustrates that carbon fiber is removed in the form of a longitudinal fracture. The reason may be is the wire electrode keeps moving forward and continuously discharging on the workpiece surface. Figure 14c shows that the recast layer forms on the machined surface. Its analysis is in the subsequent sections.

From Fig. 15a, it can be seen that some columnar structure forms in the machined surface. Figure 15b implies that transverse and longitudinal fracture of carbon fiber occurs in the process of material removal. Because the cut direction of the wire electrode is perpendicular to 0° fiber, the wire electrode is always in contact with carbon fiber along its length direction, as shown in Fig. 15d. In this case, the longitudinal fracture of carbon fiber plays a dominant role, but transverse fracture plays a secondary role in the material removal process. From Fig. 15c, it is observed that interfacial debonding comes into being and the recast layer is generated. The formation of interfacial debonding can be attributed to that wire electrode that first comes into contact with the SiC in preference to the carbon fiber during the process of spark discharge. This two different attribute material can lead to a slightly out-of-step deformation. When the stress produced by the discordant micro-deformation exceeds the interfacial strength of fiber/SiC matrix, the initial interfacial debonding starts to occur.

Figure 16 represents the surface morphology and material removal progress using machining direction B. It can be seen that the direction B is perpendicular to the fiber orientation.

That is to say, the wire electrode cuts 90° carbon fiber along a radial direction which is also illustrated from Fig. 14d. In view of this, transverse fracture of this 90° carbon fiber plays a dominant role during the material removal process. It can be seen from Fig. 16a–c that the interfacial debonding of fiber/SiC also produces due to the discordant micro-deformation between fiber and SiC. Figure 16a also shows that there are pits and melt formed during discharging on the machined surface. The melt has not completely covered on the whole surface. An obvious phenomenon can be observed in Fig. 16b that there are many micro cracks occurring in the carbon fiber,

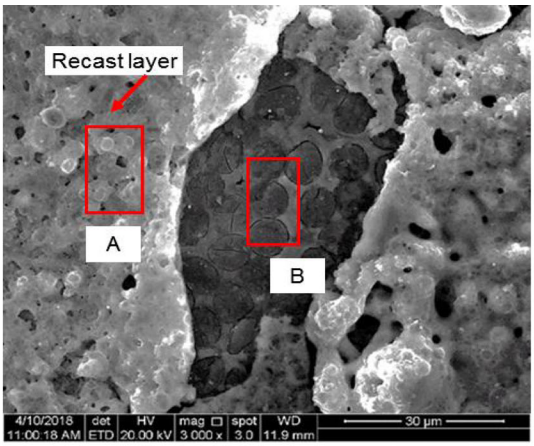

(a) SEM of the machined surface

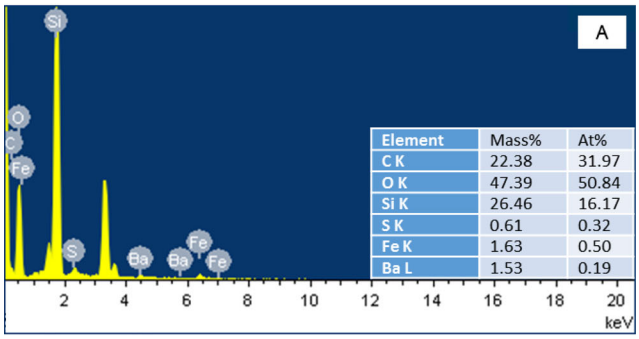

(b) EDS for region A

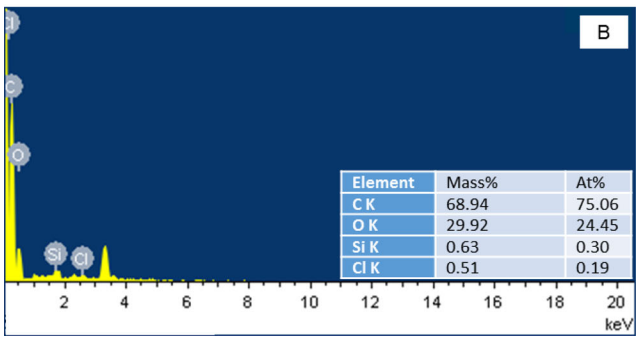

(c) EDS for region B

Fig 17 SEM of the machined surface and related EDS in WEDM of C/SiC composite. **a** SEM of the machined surface. **b** EDS for region A. **c** EDS for region B

and part of the micro cracks was cross. A few cracks also produce in the matrix surface. The formation of the micro cracks can also be explained from the thermal expansion and local microburst due to the discharged energy, which produces strong shock waves that spread around from the carbon fiber center when the wire electrode moves into the middle of the 90° carbon fiber along radial direction during discharge. Then, very high temperatures are generated at the discharged micro-region. In addition, micro cracks in the carbon fiber are also attributed to the uneven contraction of fiber along the radial direction during high-temperature carbonization of the fiber. Then the radial stress is generated which will constrain cracks producing to eliminate the concentrated stress. As shown in Fig. 16c, the alveolate recast layer forms.

Figure 17a represents the morphology machined surface in WEDM of C/SiC composite. It is observed that machined surface is carpeted with the recast layer which broadly presents a nipple shape. The cause might be that carbon dioxide is produced in the recast layer by the action of carbonization. Figure 17b and c show the EDS analysis of region A of recast layer and region B of the machined surface without the recast layer, respectively. By comparing Fig. 17b and c, it can be seen that the Fe and Ba are detected on the recast layer and not on the machined surface without a recast layer. The possible reason is that some Fe and Ba from molybdenum wire diffuse into the recast layer during the WEDM process. It also can be seen that the mass percentage of Si and O on the recast layer is higher than that on the machined surface without the recast layer. It can be inferred that iron silicide and oxygen compounds may be produced in the recast layer by the combination reaction in WEDM process. In addition to this, it is observed in Fig. 17b that partially removed carbon fiber is left in the recast layer.

4 Conclusions

(1) As the peak current increases, the machining speeds increase for two machining directions A and B. The machining speed is slower in WEDM of C/SiC composite than that of a traditional metal material. The fiber orientation effect on machining speed plays a weaker role in the WEDM of a 2D C/SiC composite.

(2) Under machining direction A, at the pulse width of 60 us, the pulse interval of 4 ns, and the number of tubes of 10, the machining speed can get a larger value. For the machining direction B, the electrical parameters are the pulse width of 20 us, the pulse interval of 4 ns, and the number of tubes of 10. For machining speed, the number of tubes and the pulse interval have no interaction for both of the machining directions A and B.

(3) In general, the surface roughness firstly increases at a small peak current and then decreases as the peak current

increases at both machining directions (A, B). The pulse width has a significant effect on the surface roughness. For the surface roughness, the number of tubes and the pulse interval have an obvious interaction at both machining directions (A, B). The fiber orientation has a larger influence degree on the surface roughness than that on machining speed in WEDM of this composite.

(4) The carbon fibers are removed in the form of transverse and longitudinal fracture. Whether the longitudinal fracture or the transverse fracture of carbon fiber plays a dominant role depends on the machining direction relative to 0°or 90° fiber orientations in the material removal process. Interfacial debonding of carbon fiber/SiC matrix also produces. Pit and recast layer generate on the WEDM surface. There are many micro cracks occurring in the carbon fiber, and part of the micro cracks was cross.

Funding information This study was funded by the Natural Science Foundation of China (grant number 51505434); the Natural Science Foundation of Henan Province (grant numbers 182300410215 and 182300410170); the Henan Province's Scientific and Technological Project (grant number 172102210547); and Henan Province's University Education Department Program for Innovative Research Team (in Science and Technology) (18IRTSTHN015).

Compliance with ethical standards

Conflict of interest The authors declare that they have no conflict of interest.

References

1. Lu ZL, Lu F, Cao JW, Li DC, Lian YY, Miao K, Jing H (2013) Fabricating hollow turbine blades using short carbon fiber-reinforced SiC composite. Int J Adv Manuf Technol 69(1–4): 417–425
2. Zhang Y, Zhang LT, He JY, Chen C, Cheng LF, Liu YS (2018) Modelling shear behaviors of 2D C/SiC z-pinned joint prepared by chemical vapor infiltration. Ceram Int 44(6):6433–6442
3. Liu Q, Huang GQ, Xu XP, Fang CF, Cui CC (2017) A study on the surface grinding of 2D C/SiC composites. Int J Adv Manuf Technol 93(1):1–9
4. Ghafarizadeh S, Chatelain JF, Lebrun G (2016) Finite element analysis of surface milling of carbon fiber-reinforced composites. Int J Adv Manuf Technol 87(1–4):1–11
5. He YL, Qing HN, Zhang SG, Wang DZ, Zhu SW (2017) The cutting force and defect analysis in milling of carbon fiber-reinforced polymer (CFRP) composite. Int J Adv Manuf Technol 93(2):1–14
6. Shan CW, Dang J, Yan JQ, Zhang X (2017) Three-dimensional numerical simulation for drilling of 2.5D carbon/carbon composites. Int J Adv Manuf Technol 93(5–8):2985–2996
7. Tang WL, Chen Y, Yang HJ, Wang H, Yao Q (2018) Numerical investigation of delamination in drilling of carbon fiber reinforced polymer composites. Appl Compos Mater:1–21
8. Ha CS, Son EJ, Cha JH, Kang MC, Lee HJ (2017) Energy-controlled micro electrical discharge machining for an Al_2O_3-carbon nanotube composite. J Electr Eng Technol 12(6):1921–1718
9. Ninz P, Landfried R, Kern F, Gadow R (2015) Electrical discharge machining of metal doped Y-TZP/TiC nanocomposites. J Eur Ceram Soc 35(14):4031–4037
10. Kumar SV, Kumar MP (2015) Machining process parameter and surface integrity in conventional EDM and cryogenic EDM of Al-SiC_p, MMC. J Manuf Process 20:70–78
11. Saxena KK, Agarwal S, Khare SK (2016) Surface characterization, material removal mechanism and material migration study of micro EDM process on conductive SiC. Procedia Cirp 42:179–184
12. Wang JJ, Zhang JF, Feng PF (2017) Effects of tool vibration on fiber fracture in rotary ultrasonic machining of C/SiC ceramic matrix composites. Compos Part B 129:233–242
13. Saxena KK, Srivastava AS, Agarwal S (2015) Experimental investigation into the micro-EDM characteristics of conductive SiC. Ceram Int 42(1):1597–1610
14. Wu ML, Ren CZ, Xu HZ (2016) Comparative study of micro topography on laser ablated C/SiC surfaces with typical unidirectional fibre ending orientations. Ceram Int 42(7):7929–7942
15. Ding K, Fu YC, Su HH, Chen Y, Yu XH, Ding GZ (2014) Experimental studies on drilling tool load and machining quality of C/SiC composites in rotary ultrasonic machining. J Mater Process Technol 214(12):2900–2907
16. Ji RJ, Liu YH, Zhang YZ, Cai BP, Ma JM, Li XP (2012) Influence of dielectric and machining parameters on the process performance for electric discharge milling of SiC ceramic. Int J Adv Manuf Technol 59:127–136
17. Liu YS, Wang CH, Li WN, Yang XJ, Zhang Q, Cheng LF, Zhang LT (2014) Effect of energy density on the machining character of C/SiC composites by picosecond laser. Appl Phys A Mater 116(3): 1221–1228
18. Zhang LF, Ren CZ, Ji CH, Wang ZQ, Chen G (2016) Effect of fiber orientations on surface grinding process of unidirectional C/SiC composites. Appl Surf Sci 366:424–431
19. Diaz OG, Axinte DA (2017) Towards understanding the cutting and fracture mechanism in ceramic matrix composites. Int J Mach Tools Manuf 118–119:12–25
20. Wang Y, Sarin VK, Lin B, Li H, Gillard S (2016) Feasibility study of the ultrasonic vibration filing of carbon fiber reinforced silicon carbide composites. Int J Mach Tools Manuf 101:10–17
21. Liao ZR, Axinte DA (2016) On chip formation mechanism in orthogonal cutting of bone. Int J Mach Tools Manuf 102:41–55
22. Du JG, Ming WY, Ma J, He WB, Cao Y, Li XK, Liu K (2018) New observations of the fiber orientations effect on machinability in grinding of C/SiC ceramic matrix composite. Ceram Int 44(12): 13916–13928